1 Introduction

Recently, a new class of rotor-synchronized pulse sequences, denoted $\mathrm{R}N_n^\nu$ was described[1,2] which are characterized by the three integer symmetry numbers N, n and ν. The symmetry theory of these pulse sequences is used to design pulse sequences which implement zero-quantum homonuclear dipolar recoupling, while decoupling isotropic chemical shifts and chemical shift anisotropies in first order average Hamiltonian theory.[3] Supercycles and composite pulses are employed to improve the robustness of these sequences with respect to chemical shifts.

We identify sequences which prove to be good candidates for operation at high spinning frequencies and magnetic fields. These sequences are compared with existing zero-quantum recoupling sequences by numerical simulations. The new sequences are demonstrated experimentally by obtaining longitudinal magnetization transfer curves for $[^{13}C_2, ^{15}N]$-glycine and by acquiring 2D homonuclear correlation spectra of [U-^{13}C]-tyrosine.

2 Pulse Sequence Symmetries

Figure 1 shows one possible construction scheme for an $\mathrm{R}N_n^\nu$ sequence, where $\tau_r = 2\pi/\omega_r$ is the rotational period and ω_r is the angular spinning frequency. The basic element $\mathscr{R}$ rotates the spins by 180° round the x-axis. The first order average Hamiltonian components obey the following selection rules:

$$\bar{H}_{lm\lambda\mu} = 0 \qquad \text{if} \qquad m\,n - \mu\,\nu \neq \frac{N}{2} Z_\lambda \tag{1}$$

where λ, μ, l and m are the spin rank, spin component, space rank and space component of the spin interaction. The integer Z_λ has same parity as λ.

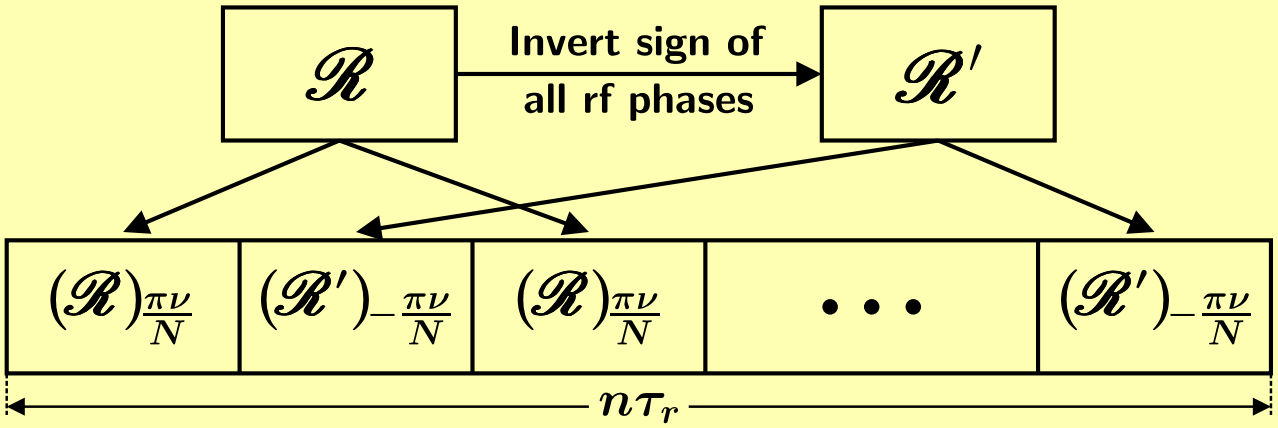

Figure 1

SSS Diagram of $R6_6^2$

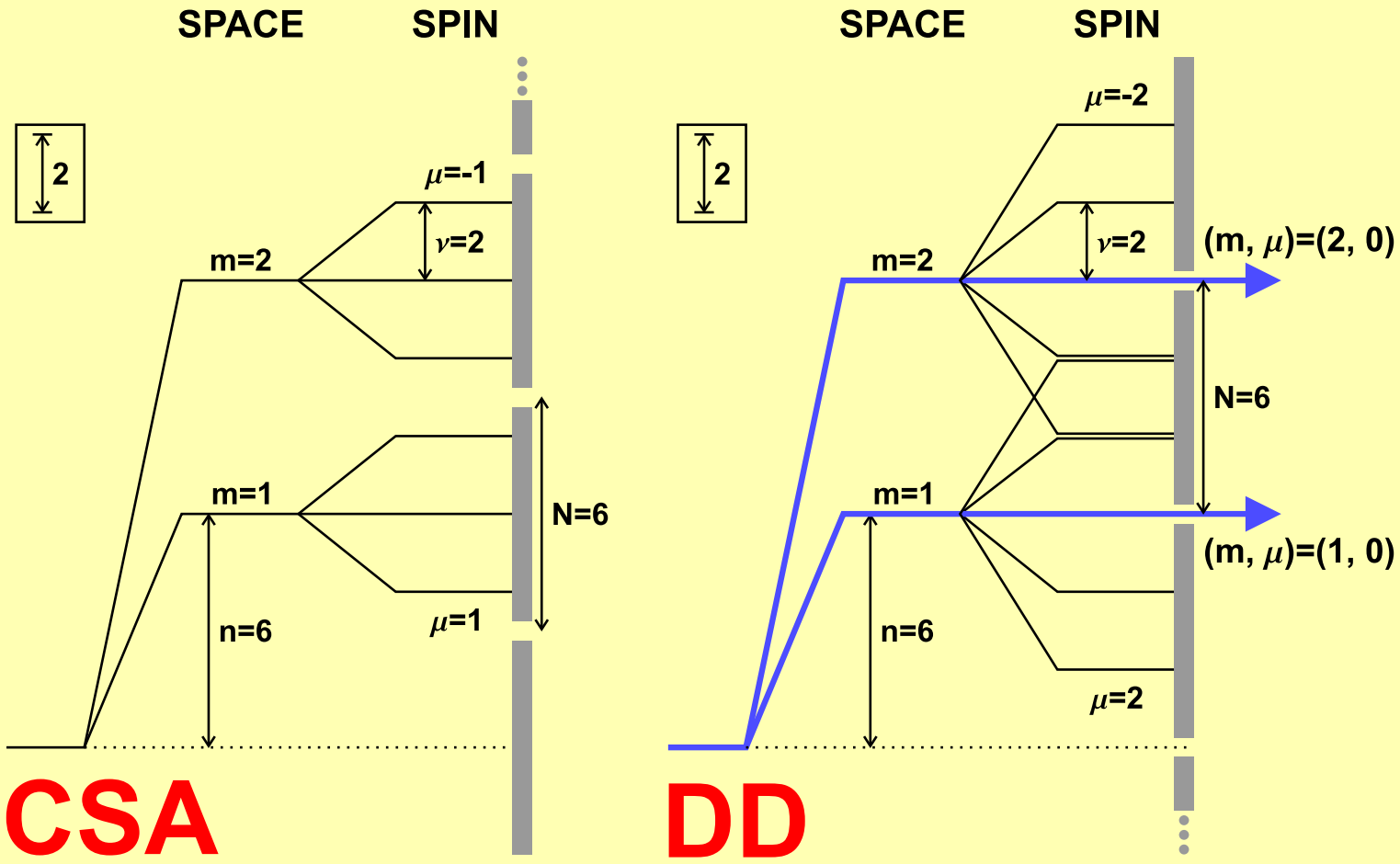

Figure 2

3 Homonuclear Zero-Quantum Recoupling

We used the symmetry principle Eq. (1) to design zero-quantum homonuclear recoupling sequences, which recpouple the homonuclear dipolar coupling terms with quantum numbers $(l, m, \lambda, \mu) = \{(2, 1, 2, 0), (2, -1, 2, 0), (2, 2, 2, 0), (2, -2, 2, 0)\}$ in the first order average Hamiltonian. Possible solutions include $\mathbf{R4}_4^1$, $\mathrm{R6}_6^1$, $\mathbf{R6}_6^2$, $\mathrm{R4}_8^1$, $\mathrm{R8}_8^1$ and $\mathrm{R8}_8^3$.

The widely used RFDR pulse sequence[5] (with the XY-4 phase cycle) corresponds to the symmetry $\mathbf{R4}_4^1$. Recently, Ishii[4] has given a symmetry based analysis of RFDR with finite rf pulses and proposed the use of symmetries such as $\mathbf{R4}_4^1$ and $\mathbf{R6}_6^2$. However, the results described here are more general and the performance of these sequences is stabilized by implementing more complex basic elements $\mathscr{R}$ and supercycles.

Figure 2 shows the space-spin selection diagram (SSS diagram) for the sequence $\mathbf{R6}_6^2$. All CSA components are suppressed and only dipolar coupling components corresponding to homonuclear zero-quantum recoupling are symmetry allowed.

4 Supercycles

Figure 3(a) shows simulations of magnetization transfer between the CO and C^{α} sites in glycine (without the J-coupling) for different supercycles of $R6_6^2$ with the basic element $\mathscr{R} = 90_{180}270_0$. Solid line: basic $R6_6^2$ sequence without chemical shifts. Dashed lines: Simulations including both isotropic and anisotropic chemical shifts, using the basic $R6_6^2$ sequence, the $R6_6^2R6_6^{-2}$ and the $SR6_6^2$ supercycle (specified in the table below).

Sequence	Supercycle	$\mathscr{R}$
$SR4_4^1$	$[R4_4^1R4_4^{-1}]_0[R4_4^1R4_4^{-1}]_{120}[R4_4^1\ R4_4^{-1}]_{240}$	$90_{270}90_090_{90}90_090_{270}90_0$
$SR6_6^2$	$[R6_6^2R6_6^{-2}]_0[R6_6^2R6_6^{-2}]_{120}[R6_6^2\ R6_6^{-2}]_{240}$	$90_{180}270_0$

The RFDR sequence with the XY-8 phase cycle corresponds to the supercycle $R4_4^1R4_4^{-1}$. The RFDR sequence with the XY-16 phase cycle corresponds to the supercycle $[R4_4^1R4_4^{-1}]_0[R4_4^1R4_4^{-1}]_{180}$.

a Supercycles

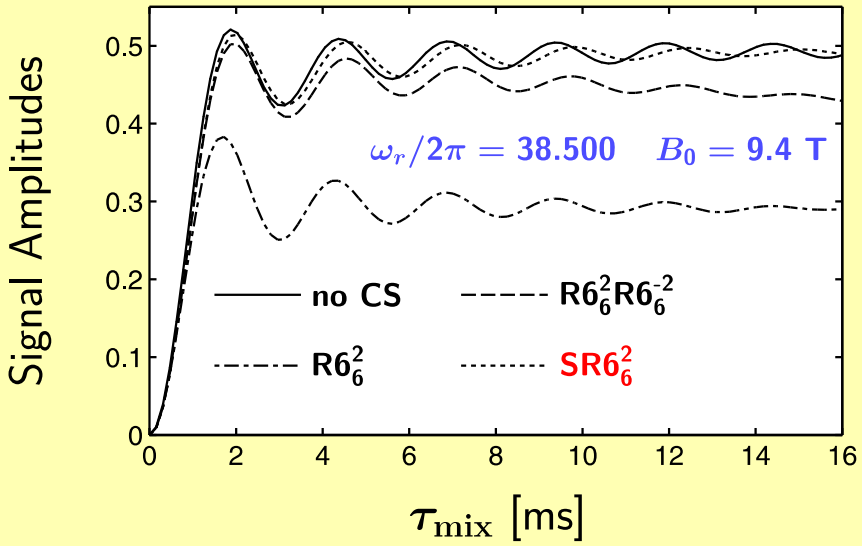

b Pulse Sequence

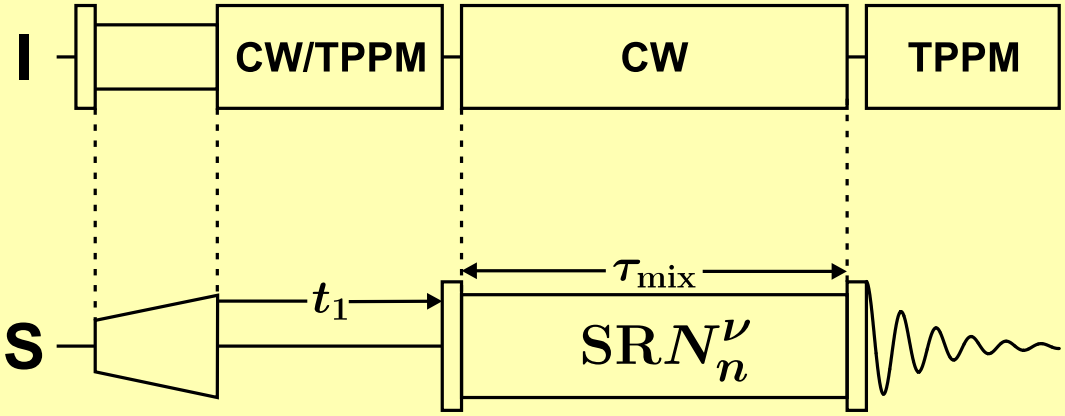

Figure 3

Exchange Curves for CO and C^{α} in Glycine

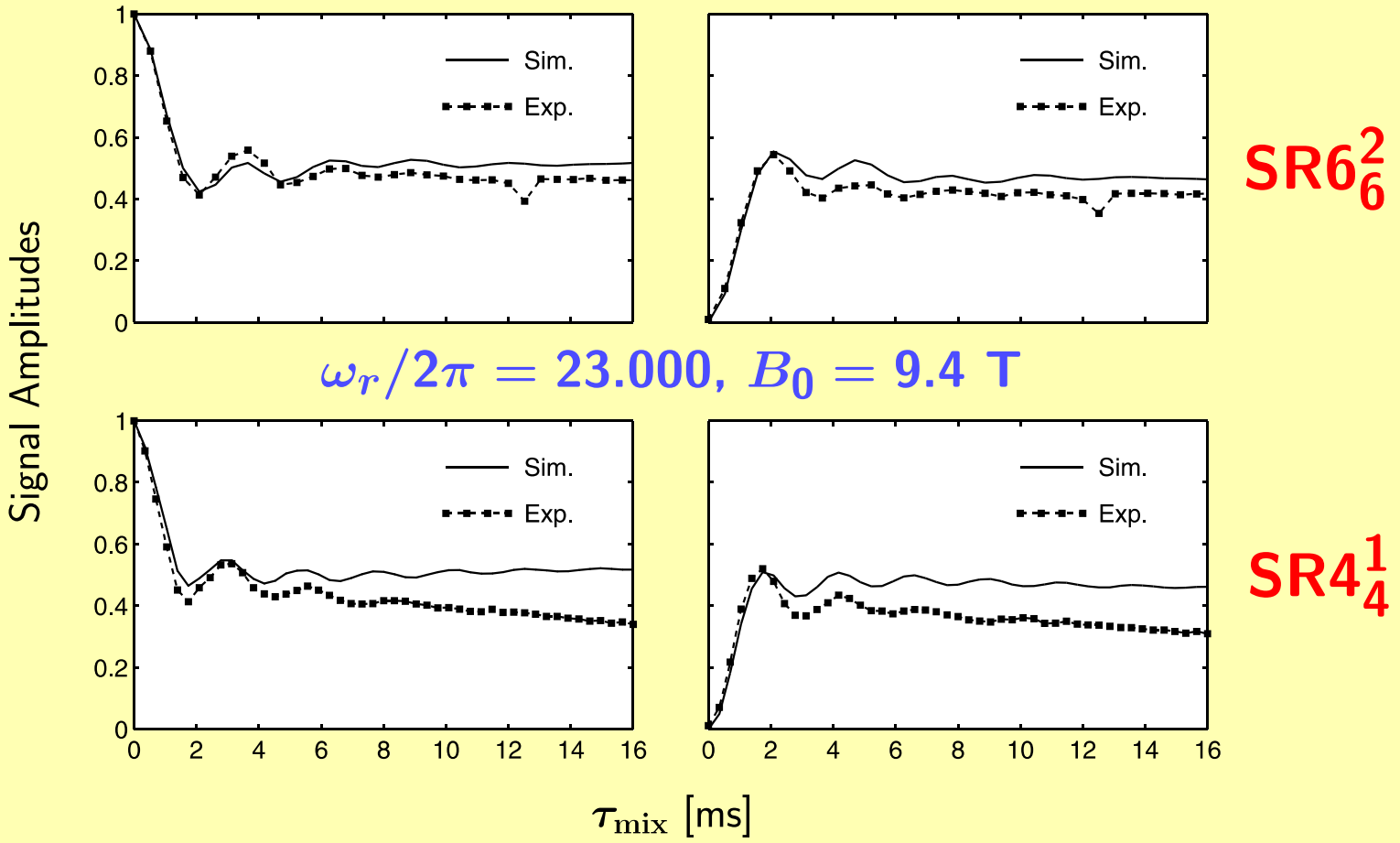

Figure 4

5 Experimental Exchange Curves for Longitudinal Magnetization

Figure 4 shows experimental longitudinal magnetization transfer curves for $[^{13}C_2, ^{15}N]$-glycine obtained with the pulse sequence shown in Fig. 3(b). Longitudinal magnetization on the CO site is prepared by the appropiate choice of t_1. During the SRN_n^ν sequence of duration τ_{mix} longitudinal magnetization is transferred between the CO and the C^α site.

The solid lines in Fig. 4 are the results of accurate two-spin simulations using the spin interaction parameters of glycine. The simulations do not take into account the relaxation during the recoupling sequence. The numerical simulations reflect the oscillations in the experimentally acquired curve rather well. The relaxation loss during the recoupling sequence is slightly higher during the $SR4_4^1$ sequence compared to the $SR6_6^2$ sequence. This is due to the fact that the mismatch between the ^1H and ^{13}C nutation frequencies of rf fields during the recoupling sequence is higher in the case of the $SR6_6^2$ sequence.

6 Simulations of ^{13}C Magnetization Transfer

Figures 6–8 show simulations of magnetization transfer as a function of the mixing time τ_{mix} and the static magnetic field B_0 for three representative spin pairs. All spin interactions (J-couplings, isotropic and anisotropic chemical shifts) were included in the simulations. The choice of the spectrometer reference frequency and the isotropic chemical shifts for the three cases are shown in Fig. 5.

These three cases represent the different scenarios if ^{13}C correlation spectroscopy is performed to obtain a complete ^{13}C spectrum in peptides and proteins.

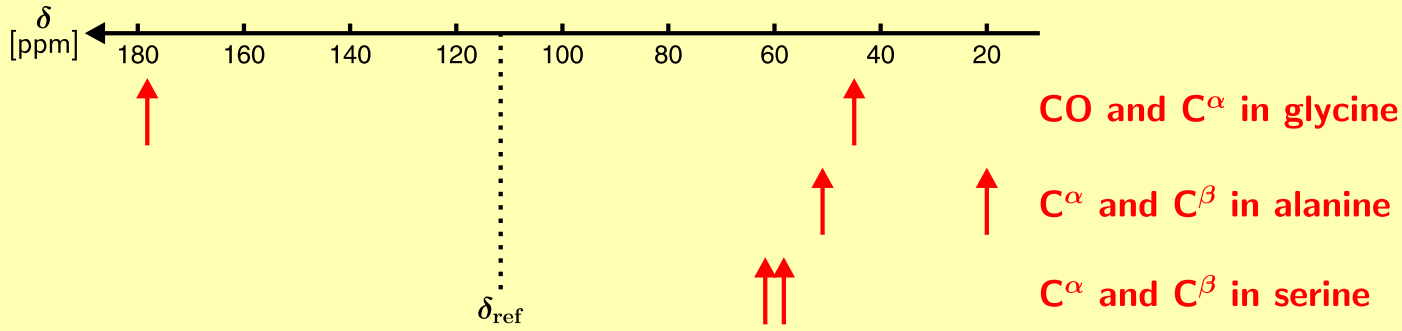

Figure 5

CO and C^{α} in Glycine

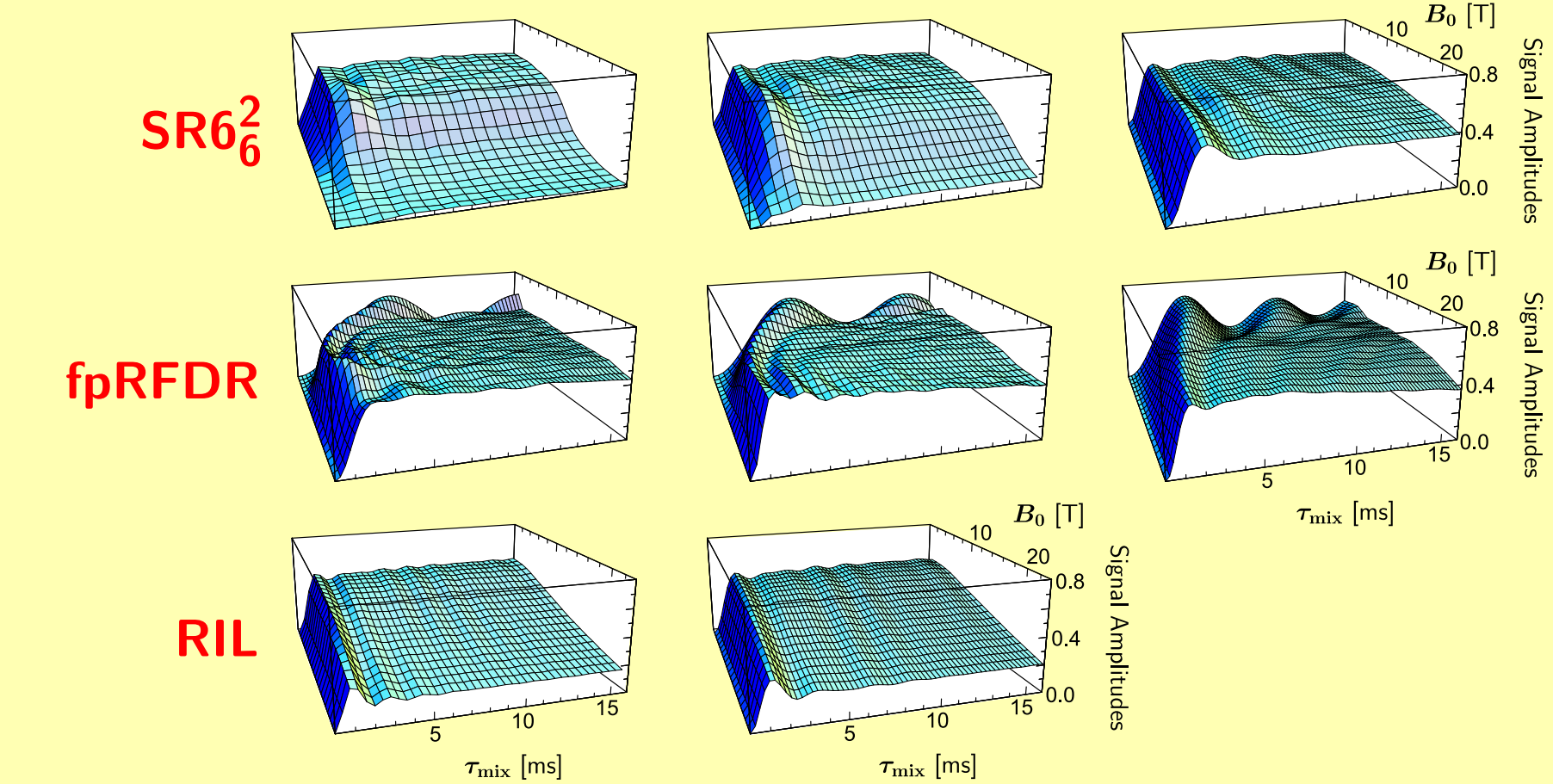

Figure 6

C^{α} and C^{β} in Alanine

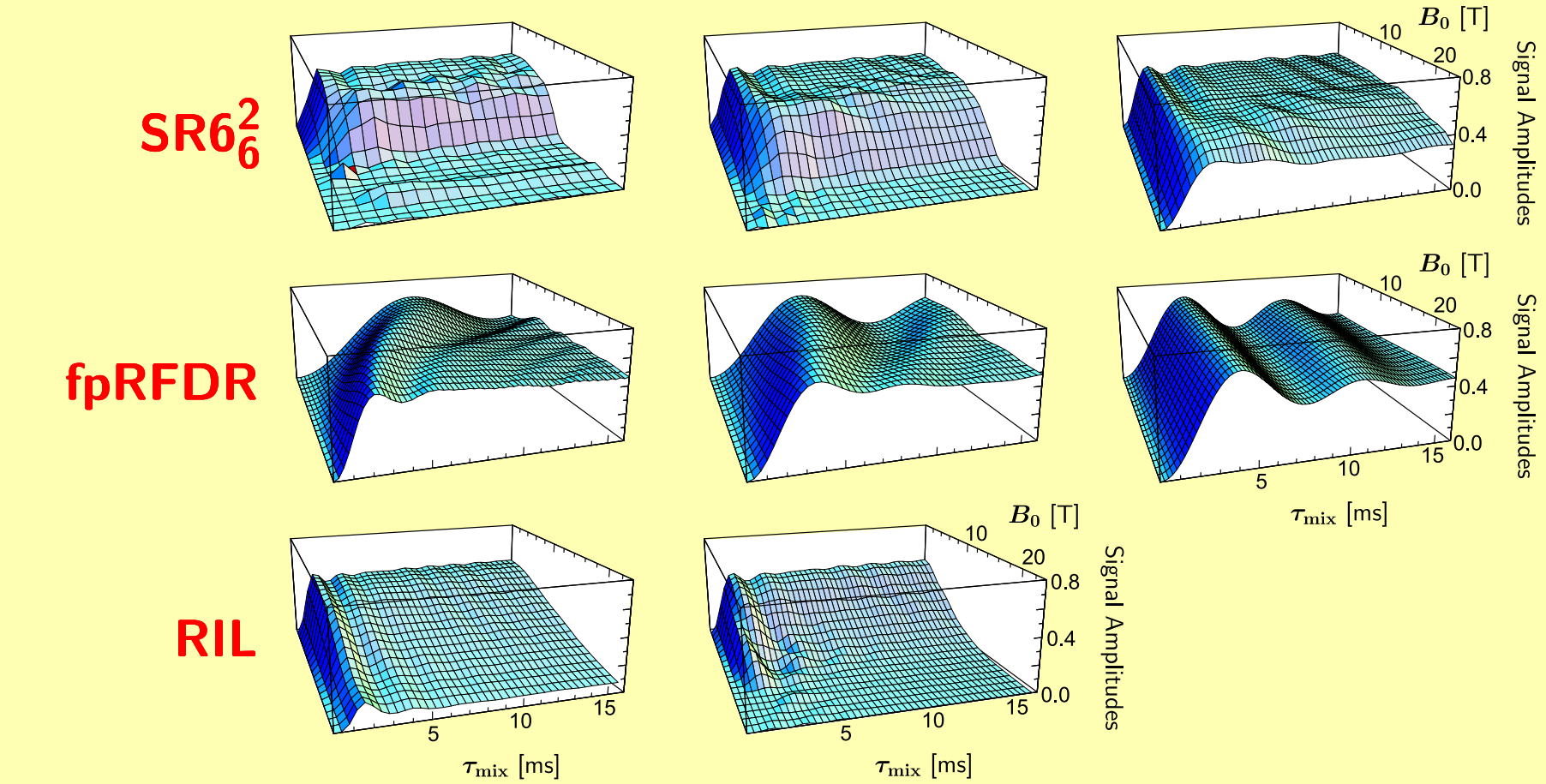

Figure 7

C^{α} and C^{β} in Serine

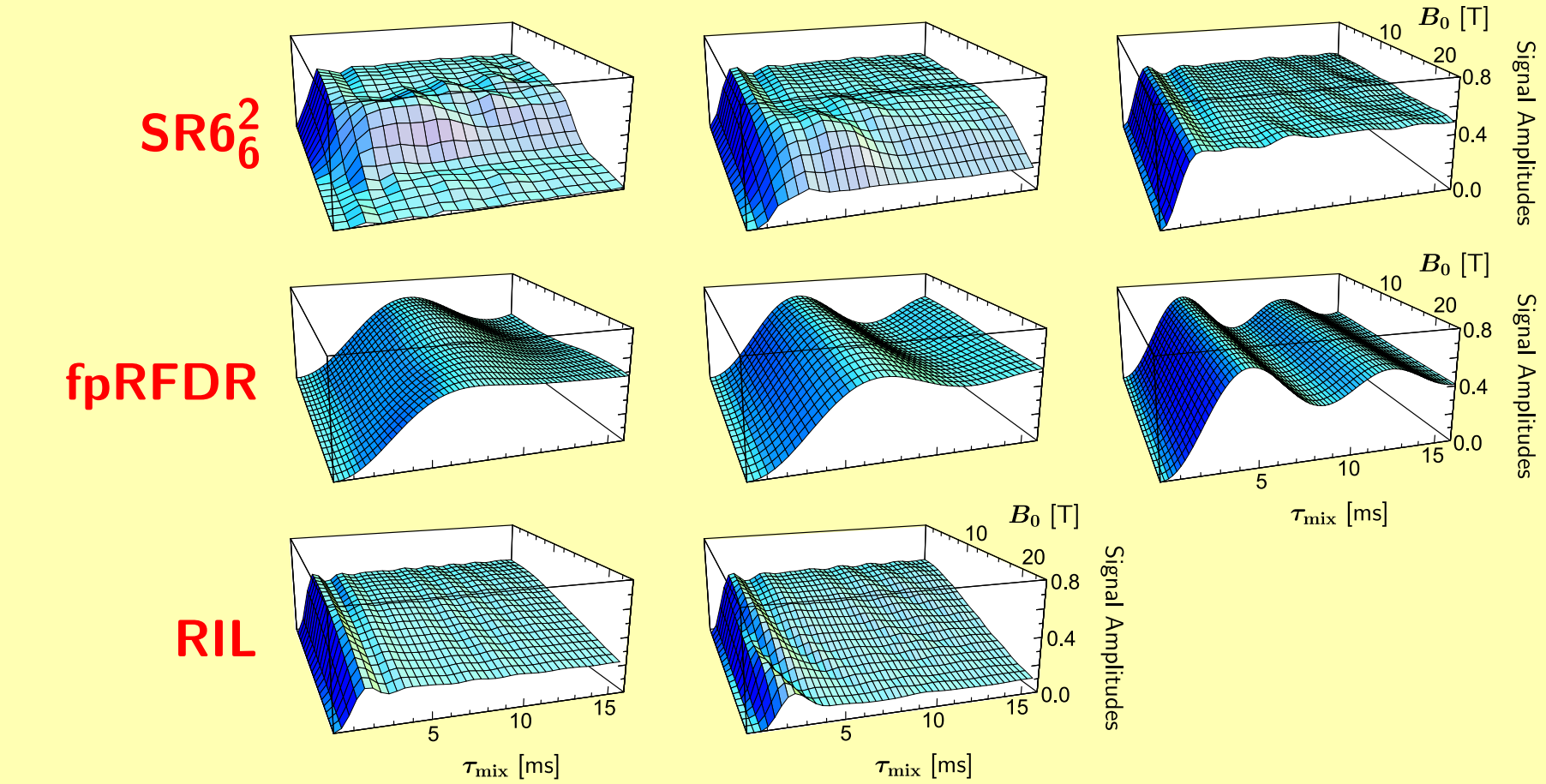

Figure 8

7 Experimental Homonuclear Correlation Spectra

Figure 9 shows experimental two-dimensional homonuclear chemical shift correlation spectra obtained with the pulse sequence shown in Fig. 3(b) on a sample of [U-^{13}C]-tyrosine (Fig. 9). The spectra were acquired using the SR6$_6^2$ sequence at a field 9.4 T, spinning frequency of 23.000 kHz and mixing intervals of 1.0 and 9.9 ms.

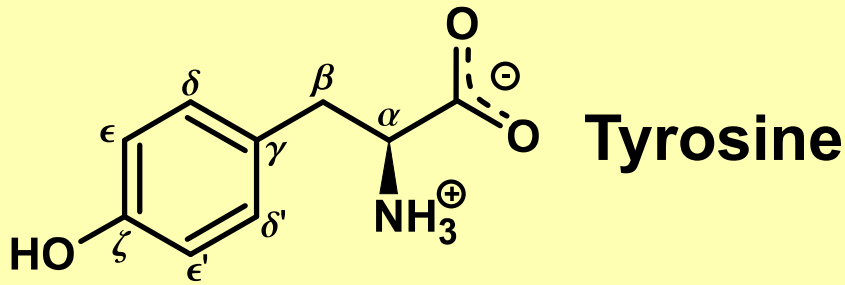

Figure 9

$\tau_{mix} = 1.0$ ms

$\tau_{mix} = 9.9$ ms

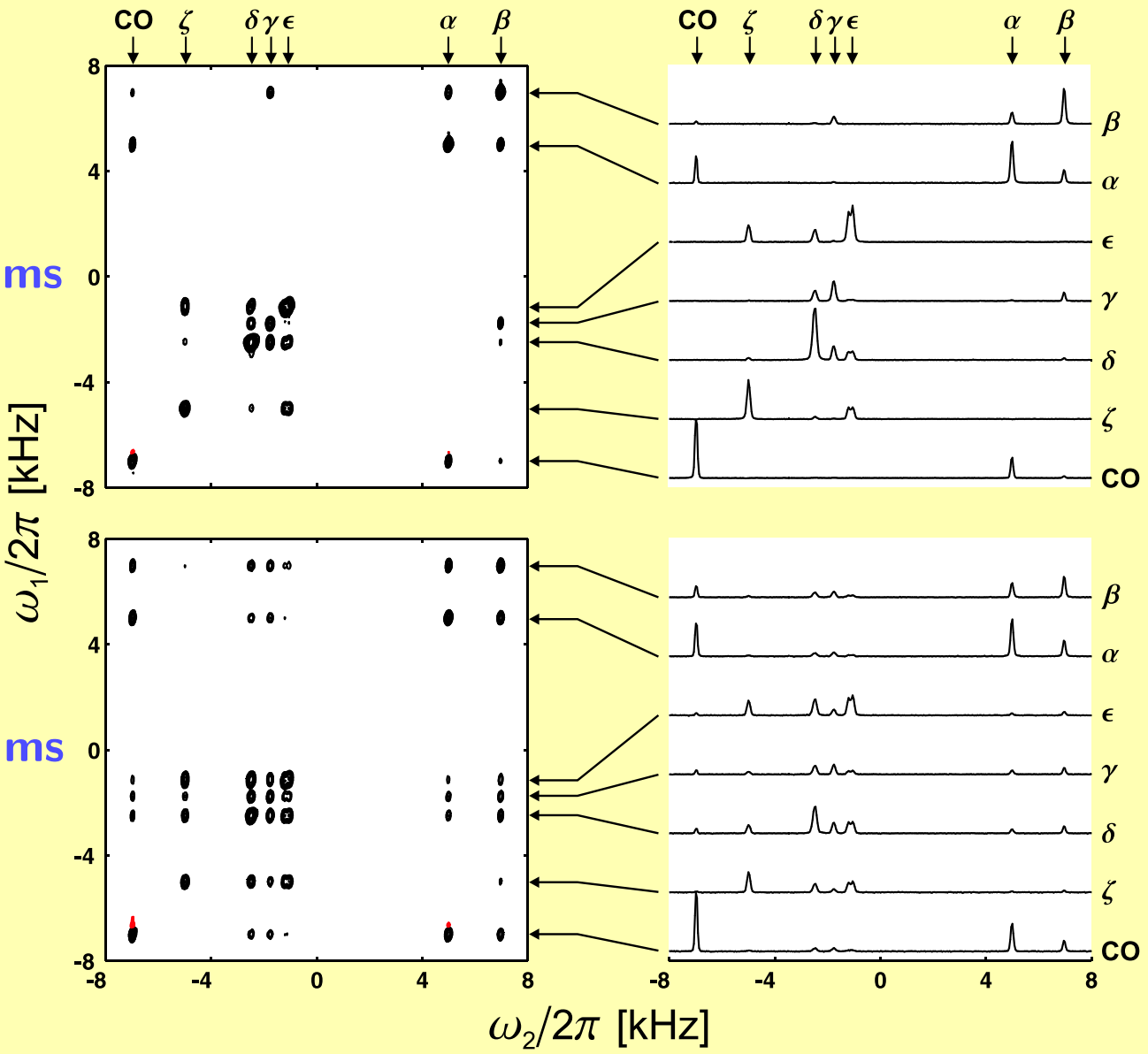

$\mathbf{SR6_6^2}$

$\omega_r/2\pi = 23.000$

$B_0 = 9.4$ T

Figure 10

8 Conclusions

We showed how symmetry arguments may be used to construct zero-quantum homonuclear recoupling sequences in MAS solid-state NMR.

The performance of these sequences is stabilized by implementing composite pulses as basic elements and supercycles. One of the most promising candidates, called $\mathrm{SR6}_6^2$, is demonstrated experimentally by obtaining longitudinal magnetization transfer curves for [$^{13}C_2$, ^{15}N]-glycine and by the two-dimensional ^{13}C correlation spectroscopy of [U-^{13}C]-tyrosine, both at a spinning frequency of 23.000 kHz.

The performance of several different zero-quantum recoupling sequences has been simulated for three test cases representing conditions typical for ^{13}C correlation spectroscopy in [U-^{13}C]-labelled proteins. The $\mathrm{SR6}_6^2$ sequence gives very good performance over all currently accessible magnetic field strengths, providing the spinning frequency is very high (simulated at 38.500 kHz). At the more realistic accessible spinning frequency of 23.000 kHz, its performance is adequate for work at magnetic fields up to around 12 T.

9 Acknowledgments

The research was supported by the Göran Gustafson Foundation for Research in the Natural Sciences and Medicine, and the Swedish Natural Science Foundation. A. B. has been supported by the Marie Curie Research Training Grant ERBFMBICT961439 from the European Union. J. S. a. d. G. is supported by the Deutsche Forschungsgemeinschaft (SCHM 1570/1-1). We would like to thank O. G. Johannessen for experimental help, A. Sebald for discussions and A. Laaksonen for computer resources.

References

[1] **M. Carravetta, M. Edén, X. Zhao, A. Brinkmann, and M. H. Levitt, Chem. Phys. Lett. 321, 205 (2000).**

[2] **A. Brinkmann and M. H. Levitt, J. Chem. Phys. 115, 357 (2001).**

[3] **A. Brinkmann, J. Schmedt auf der Günne, and M. H. Levitt, in manuscript.**

[4] **Y. Ishii, J. Chem. Phys. 114, 8473 (2001).**

[5] **A. E. Bennett, J. H. Ok, R. G. Griffin, and S. Vega, J. Chem. Phys. 96, 8624 (1992).**